International Journal of Bioelectromagnetism
Vol. 6, No. 1, pp. 19-26, 2004.
www.ijbem.org

Comprehensive Assessment of Cardiac Activation and Repolarization Dynamics by Body Surface Potential Mapping

György Kozmann[a,b], Kristóf Haraszti[a,b]

[a]*Dept. of Information Systems, University of Veszprém, Veszprém, Hungary*
[b]*Dept. of Biomedical Eng., Res. Inst. for Techn. Physics and Material Sciences of Hungarian Academy of Sciences, Budapest, Hungary*

Correspondence: György Kozmann, Dept. of Information Systems, University of Veszprém, Egyetem Str. 10, H-8200 Veszprém, Hungary.
E-mail: *kozmann@mfa.kfki.hu*, phone +36 88 422022 4322, fax +36 88 422022 4320

Abstract. Several studies emphasize the utility of dynamical heart rate parameters and/or repolarization disparity in the assessment of malignant arrhythmia vulnerability. In this study the spatio-temporal action potential dynamics were assessed by the use of body surface potential map (BSPM) records. Healthy subjects and a group of arrhythmia patients were enrolled in the study. Records were taken with a typical length of 5 minutes. The spatio-temporal nature of activation and repolarization sequence was characterized by QRS and QRST integral and integral difference maps. Furthermore, RR distances, nondipolarity indices (NDI) and the angle of 192D QRS and QRST vectors were used to assess depolarization and repolarization dynamics. Results revealed that repolarization changes are causally preceded by perturbations in the depolarization process. Substantial non-overlapping information was found in the frequency spectra of the heart rate (RR) parameter and in the spatial activation and repolarization complexity, represented by NDI. Apparently, the diminished effect of respiratory arrhythmia is associated with increased repolarization dispersion. Results on the effect of premature stimuli on the repolarization dispersion show that NDI increases immediately after a single premature stimulus, though in arrhythmia patients significant NDI peaks may occur without premature stimuli as well.

Keywords: Repolarization Dynamics, QRS Integral, QRST Integral, Index of Non-Dipolarity, Heart Rate Variability

1. Introduction

According to basic electrophysiological experiments, arrhythmia vulnerability is associated with elevated disparity of ventricular repolarization. Several possible mechanisms were studied that may result in the elevation of arrhythmia vulnerability [Laurita et al., 1996; Laurita et al., 1998; Shimizu et al., 2000]. Noninvasive methods were recommended for the detection of pathological repolarization disparity, including measurements performed on low-noise averaged majority beats, time- and frequency domain heart rate variability measurements, QT dispersion estimates etc [De Ambroggi et al., 1997; Nadeau et al., 1988; Lombardi, 2000; Mitchel et al., 1996; Surawitz, 1996] These measurements assess the electrical substrate of arrhythmias based on the spatial distribution of body surface ECG signals or try to get information from the dynamics of sinus beats, as well as from the vulnerability changes evoked by single or multiple premature stimuli.

In this paper we use QRS and QRST integral maps and three scalar parameters of the subsequent beats to reveal malignant changes in a train of beats. Special attention has been paid to the variability of the normal sinus rhythm in terms of well established and recently suggested parameters emphasizing different aspects of the heart's electrical activity and the spatio-temporal dynamics evoked by premature ventricular stimuli.

1.1. Background

Based on previous theoretical studies QRS integral of an arbitrary unipolar chest surface ECG signal in point P, (P,t), is related to the (r) endo-epicardial activation sequence by Eq. 1, where z(P,r) stands for the lead field along the Fs cardiac surface [Cuppen and van Oosterom, 1984; Gulrajani, 1998]. Consequently, the QRS integral map is a lead-field weighted projection of the endo-epicardial activation sequence on the chest surface.

$$\int_{QRST} \phi(P,t)dt = -\iint_{F_T} \mathbf{z}(P,\mathbf{r})\tau(\mathbf{r})dF_T \qquad (1)$$

QRST integral maps computed from chest surface unipolar leads are associated with the volume integral of the $\Delta\mu(\mathbf{r})$ gradient of the $\mu(\mathbf{r})$ action potential area of the $\varphi(\mathbf{r}, t)$ action potentials weighted by the lead-fields corresponding to the volume elements (Eq. 2). Obviously, as long as the spatial distribution of $\mu(\mathbf{r})$ action potential areas is constant within the myocardium, QRST integrals (and QRST integral maps) are invariant to the activation sequence [Geselowitz, 1983]. Consequently, beat-by-beat application of Eq. 1 and Eq. 2 provides a noninvasive tool for the study of spatio-temporal properties of cardiac activation separately and in association [Gepstein et al., 1997].

$$\int_{QRST} \phi(P,t)dt = -k\iiint_{V_s} \mathbf{z}(P,\mathbf{r})\nabla\mu(\mathbf{r})dV_s \qquad (2)$$

where

$\mu = \int_{QRST}[\phi(\mathbf{r},t)-\phi_r(\mathbf{r})]dt$ (i.e.: area of action potential)

$\varphi_r(\mathbf{r})$ = resting membrane potential

V_S = volume of sources (myocardium)

k = constant

2. Material and Methods

We assessed experimentally the noninvasive spatio-temporal depolarization and repolatization (activation propagation and action potential area) dynamics by the use of long BSPM records taken on healthy subjects and arrhythmia patients, with a typical length of 5 minutes. ECG signals were recorded from 64 chest positions according to the electrode layout suggested in Amsterdam.

Map data processing started with the identification of individual beats, high-precision determination of QRS fiducial points, and classification of beats according to their QRS patterns. Subsequently, Qon, Send and Tend points were marked in each heart cycle by an automatic procedure, but the final position of these points was adjusted by human intervention. For premature beats, when R waves were superimposed on the previous T waves, a special subtraction algorithm was applied for the separation of waves, similar to that discussed in [Sippensgroenewegen et al., 2001; Marenco et al., 2003]. After a linear base-line adjustment from the measured 64 signals, unipolar ECG signals were estimated in 128 un-measured chest locations of the 192-lead arrangement introduced at the CVRTI, Salt Lake City. The procedure of signal estimations followed the principle suggested by [Lux et al., 1978] Finally QRS and QRST integrals were computed from the data of the 192-lead system.

For the detailed quantitative representation of beat-by-beat spatial activation and repolarization patterns, QRS and QRST integral maps and difference maps (indicating departure from the average distributions) were drawn. The temporal dynamics were characterized in a simplified way by the time series of RR distances and the angle spanned by the 192D QRS and QRST vectors. Furthermore, the dynamics of repolarization disparity were characterized by the parameter of QRST integral map non-dipolarity index (NDI) introduced at the CVRTI.

RR, NDI and time-series were analyzed both in the time and frequency domain, by the STATISTICA program package (auto-, and cross correlation, spectral density, coherence, etc.)

Since RR, NDI and time-series are subjects to noise or inconsistencies in wave-limit determination (due to the intervention of human operator), simple reproducibility studies were performed. The results of two independent processing runs were compared visually and by the rms error.

3. Results

Measurement reproducibility values of the RR, NDI and parameters in low noise records provided relative variance (SD/M) values of 0, <0.04 and <0.02, while the higher noise clinical records yielded <0.001, <0.1 and <0.05 values, respectively. The visual comparison of the repeated integral and integral difference map computations did not detect meaningful changes in any details.

Results obtained are illustrated by typical examples for healthy subjects (Fig. 1 and Fig. 2) and arrhythmia patients (Fig. 3 and Fig. 4). Illustrations given below show the unexplored features of QRS and QRST map-dynamics and that of the parameter time-series.

The reproducibility of the results illustrated above was checked by the comparison of results gained from the same raw data by repeated processing. This type of test seems to confirm validity of our results from the point of view of signal processing.

In Fig. 5 a typical example is shown on the QRS and QRST integrals of a premature ventricular beat and the cycles preceding and following it. The map patterns of the premature beat showed a reversed character, i.e. the areas positive (red) in QRS integral turned negative (blue) in the QRST integral and vice versa.

Fig. 7 shows the time course of the RR distances, angles and NDI indices in a short epoch centered around a single premature beat with the same ectopic focus.

In our example angles of QRS and QRST vectors jumped consistently (in all the ectopic foci) from the average of 50° of sinus beats approximately to 150° or more, due to a premature stimulus.

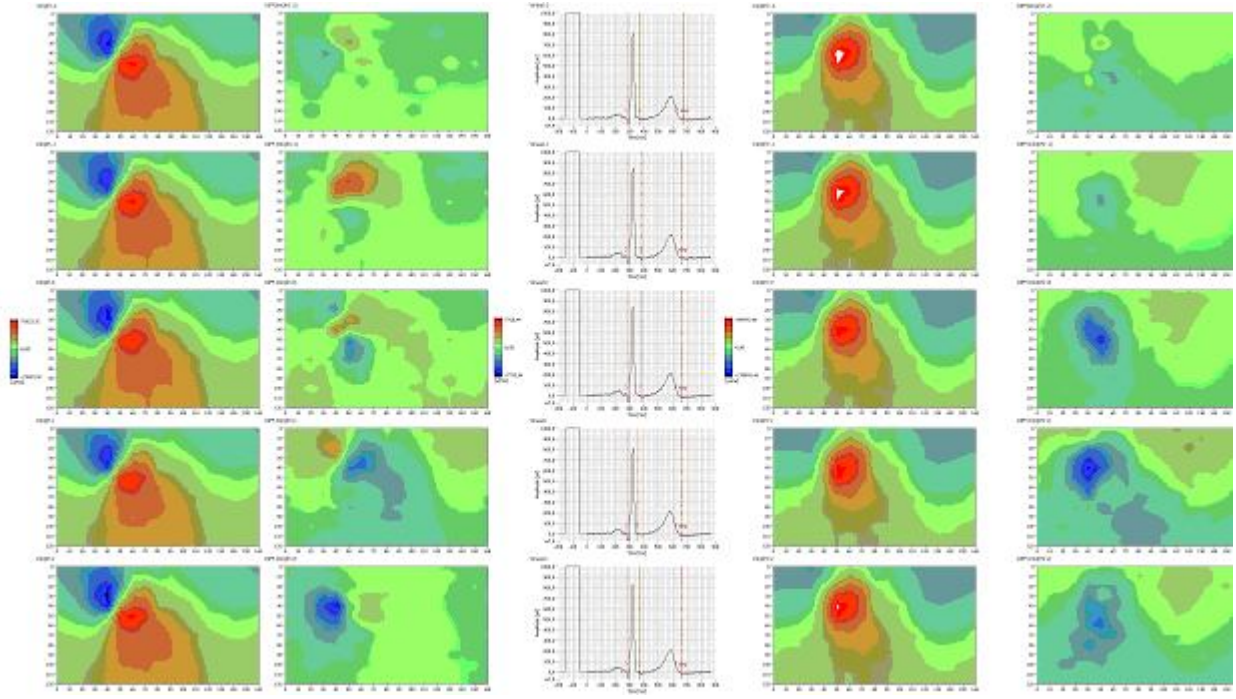

Figure 1. *Color coded QRS integral (1st column), QRS integral actual minus average (2nd column), reference ECG (3rd column), QRST integral (4th column) and QRST integral actual minus average (5th column) maps of a healthy subject in five consecutive cycles. In the chest representation, the left side of each integral map shows the anterior thoracic surface, while the right side represents the back. The scales in each column were normalized separately; subsequently the colors were symmetrically distributed*

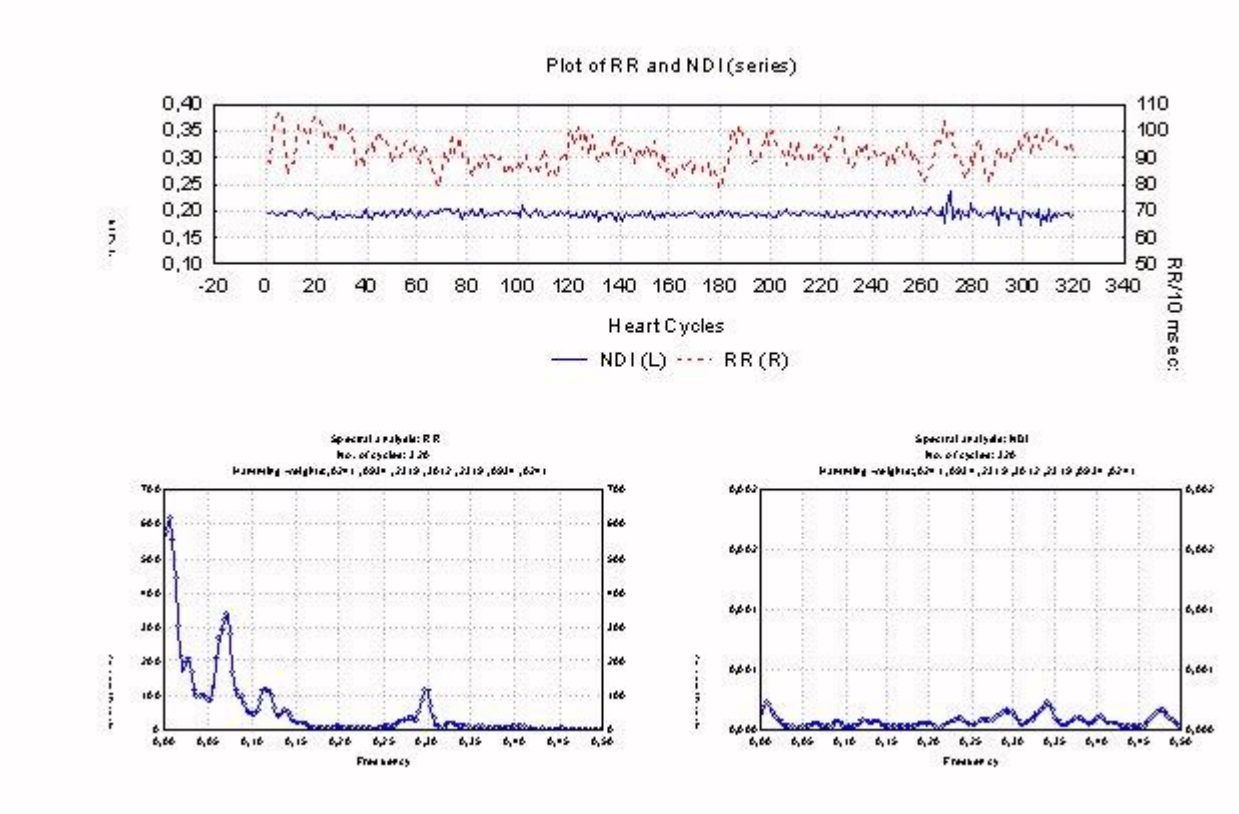

Figure 2. *Typical results of a healthy subject. Top: RR and NDI time-series, bottom left: spectral density of RR sequence, right lower: spectral density of NDI series. Spectral densities were calculated by 7 element Hamming window. (When comparing Fig. 2 and Fig. 4, consider the different scaling of the vertical axes!)*

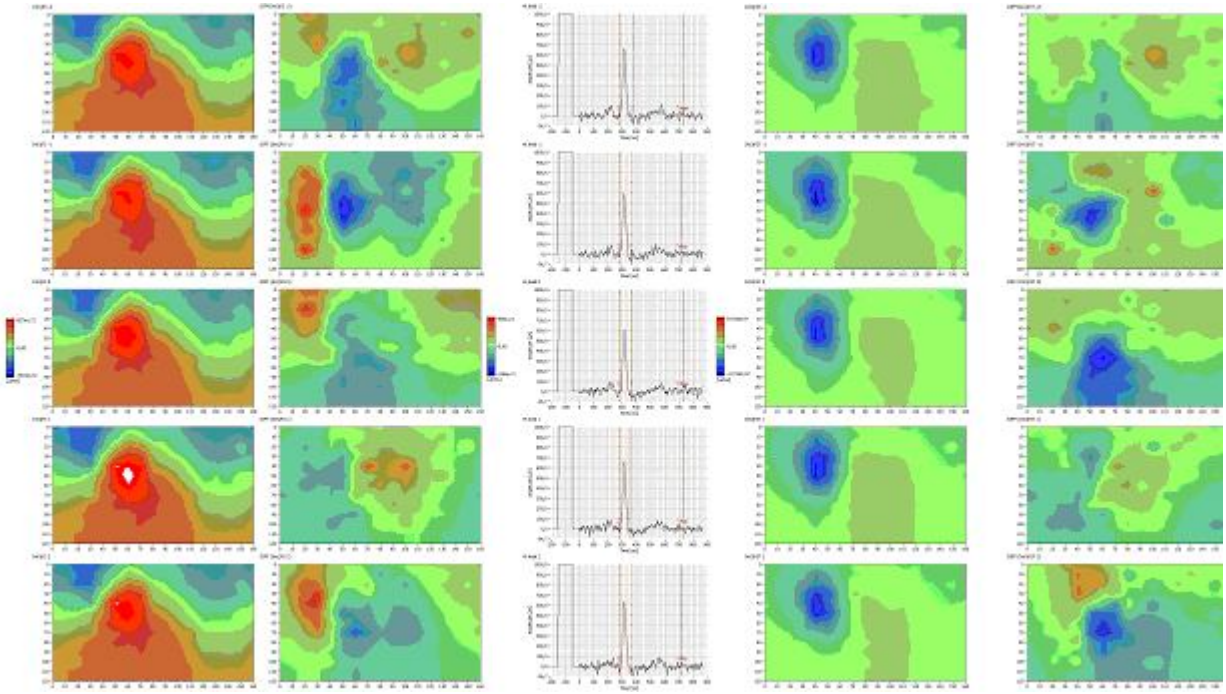

Figure 3. *Color coded QRS integral (1st column), QRS integral actual minus average (2nd column), reference ECG (3rd column), QRST integral (4th column) and QRST integral actual minus average (5th column) maps of an arrhythmia patient in five consecutive cycles. See details in the legend of Fig. 1.*

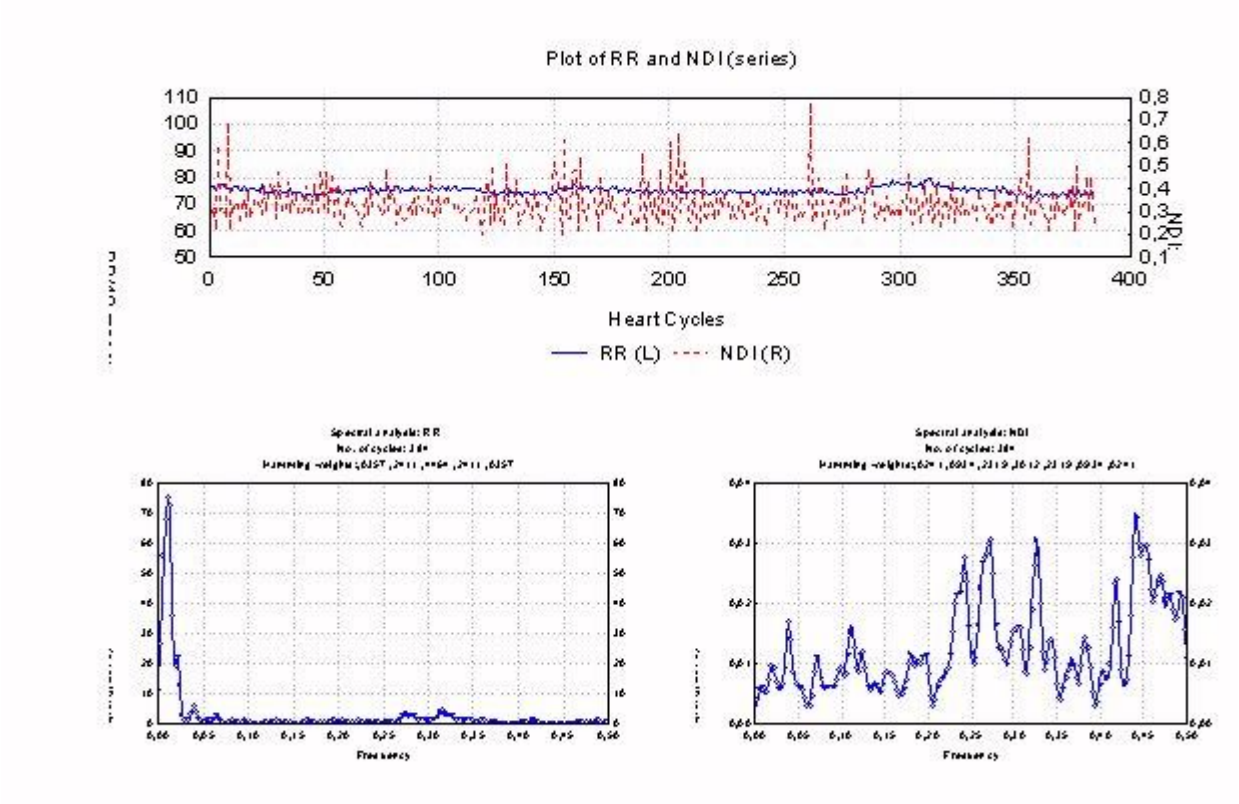

Figure 4. *Plot of RR and NDI parameters of the patient shown in Fig. 3. (From the 5 min records premature ventricular beats and the beats before and after the stimuli were excluded.) Bottom diagrams show the relevant spectral densities computed by 7 element Hamming windows. (When comparing Fig. 2 and Fig. 4 consider the different scaling of the vertical axes!)*

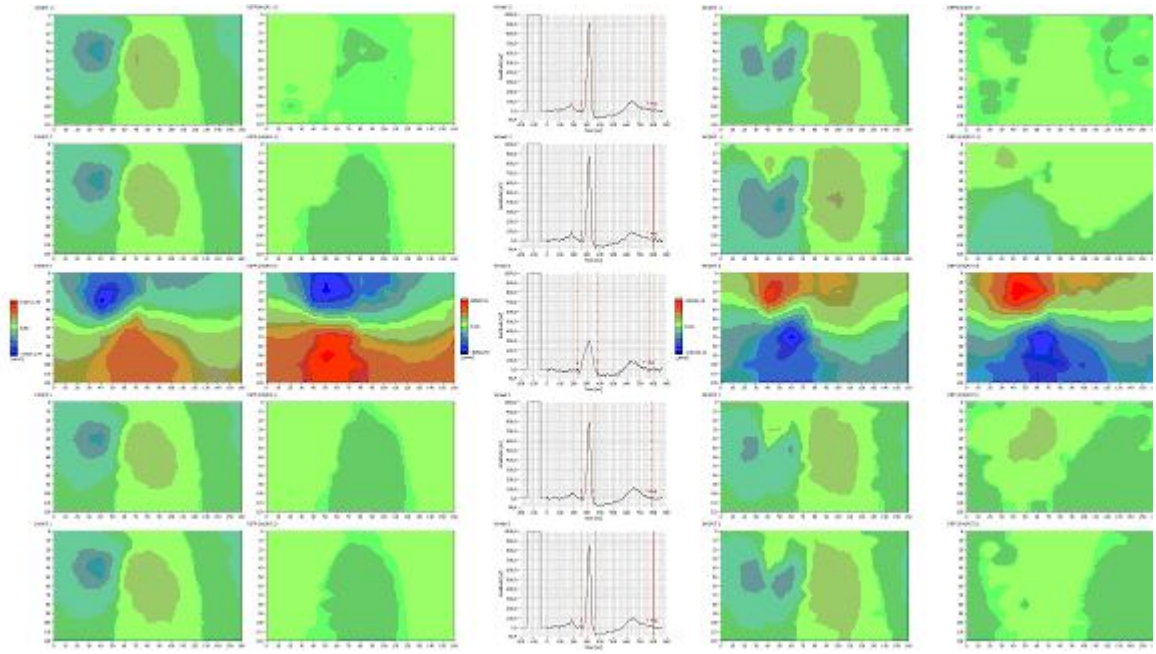

Figure 5. *Color coded QRS integral (1st column), QRS integral actual minus average (2nd column), reference ECG (3rd column), QRST integral (4th column) and QRST integral actual minus average (5th column) maps of an arrhythmia patient in five consecutive cycles. The maps of the 3rd row represent the depolarization and repolarization changes due to a single premature stimulus. See details in the legend of Fig. 1.*

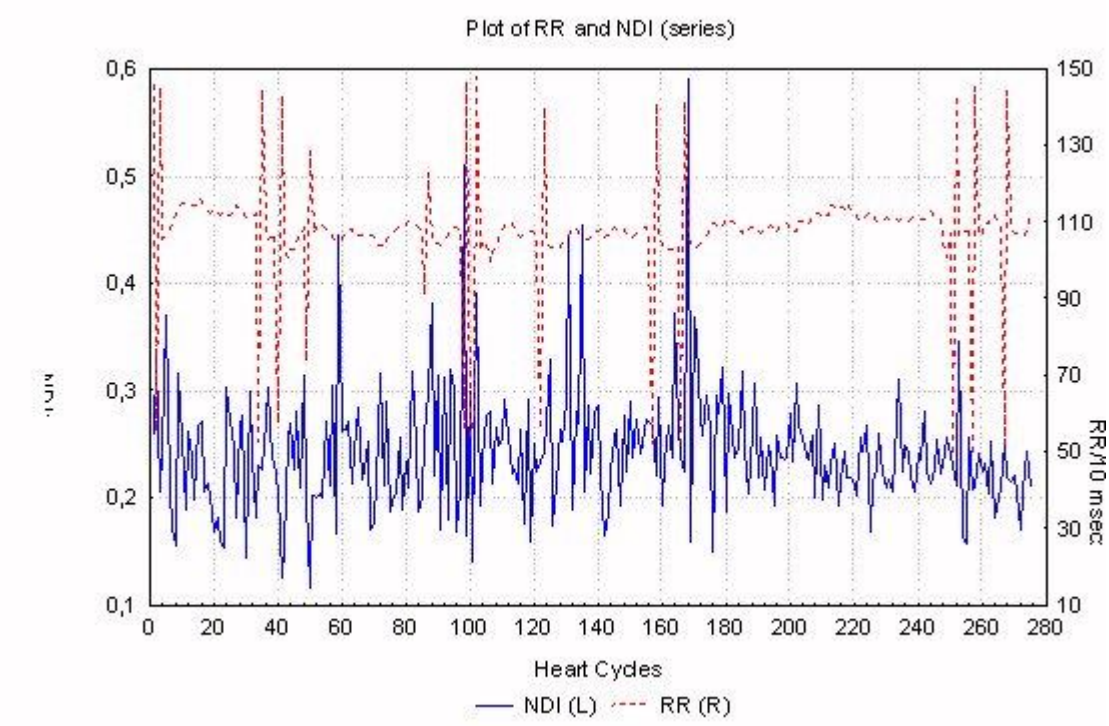

Figure 6. *Plot of the 5 min records of RR and NDI parameters of the patients shown in Fig. 5. Large deviations of RR values (red graph) denote ventricular premature beats and the compensatory pause following them. Comparison of the timing in the RR and NDI (blue) parameters show, that large NDI deviation may occur without premature stimuli as well.*

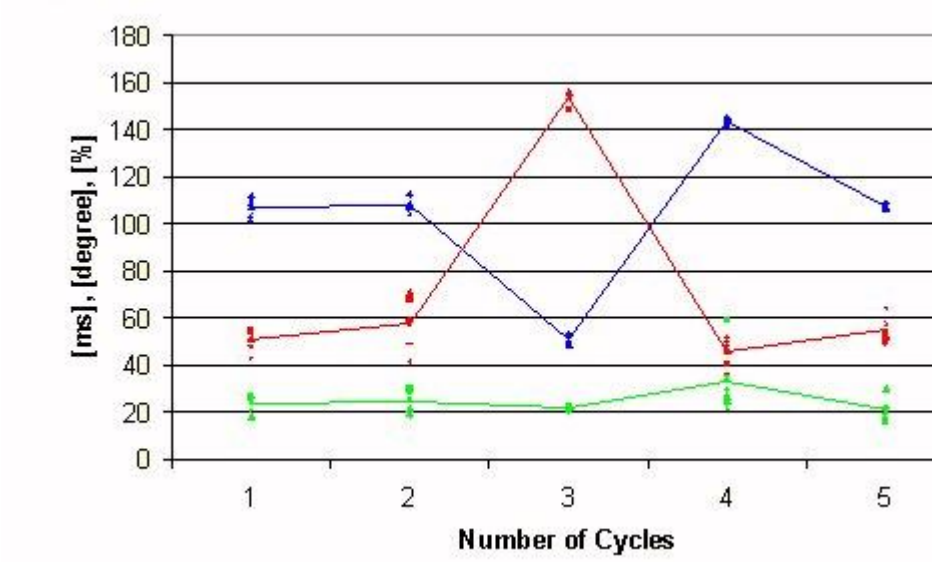

Figure 7. *Scattering of RR/10 distances, NDI and angles in five subsequent beats (centered on a premature beat). Parameter mean values are connected by polygons.(RR: blue, NDI: green, : red)*

4. Discussion

QRS and QRST integral maps of healthy subjects show a stable overall pattern along the time coordinate. However the detailed evaluation of the difference maps in the second and fifth column of Fig. 1 show QRS pattern changes typically with 10% of the amplitude range of the average maps. In the case of the QRST integral differences, the relative amplitude range is similar. The spatial pattern of the difference distributions has a considerable variability in the subsequent beats in both types of integral maps. The association of the QRS and QRST integral variations is clearly observable. Each significant change in QRS integral is accompanied by a significant change in QRST integrals and vice versa. In our arrhythmia patients the QRS integral map variability augmented slightly, but the variability of QRST integral maps increased significantly. The typical QRST variability ranges went up to 25% of the average map ranges in amplitude, or even higher. The strong association between depolarization and repolarization changes persisted, even the patterns of changes showed a clear association. Our beat-by-beat analysis confirm that repolarization changes are causally preceded by perturbations in the depolarization process, so the two phenomena should not be separated in a detailed analysis [Gepstein et al., 1997].

In normal subjects in time domain significant respiratory changes were observed in the RR intervals, while NDI and plots did not show significant fluctuations (Fig. 1). As a consequence, in frequency domain RR time-series revealed the well known characteristic LF and HF (low and high frequency) spectral peaks while very low amplitude changes were observed in NDI (i.e. QRST pattern complexity was nearly identical). However, in the 0.4 - 0.5 Hz range a frequency component higher than the respiratory frequency (peak around 0.4 Hz) was consistently present although in all of our healthy subjects those peaks were rather weak. In the group of the arrhythmia patients time-domain RR fluctuations diminished, while NDI and fluctuations increased significantly (compare the upper charts in Fig. 2 and Fig. 4). The frequency-domain analysis of these time-series clearly shows the weakening of the respiratory peak in the spectra, and the strengthening of the NDI spectral peak around 0.4 Hz, which is due to the disease. The biophysical meaning of the 0.4Hz NDI spectral peak is not properly understood at the moment, but it seems to be obvious, that this type of spatio-temporal repolarization dynamics may contain useful information not available in HRV spectra. Apparently the inadequate blood pressure control in respiratory arrhythmia is compensated by a phenomenon based on the modulation of QRS and QRST integrals, i.e. the increased variability of depolarization and repolarization dispersion.

According to previous studies [Laurita et al., 1996] premature stimuli produce significant, coupling-interval dependent alteration in dispersion of refractoriness that forms the electrophysiological basis of malignant arrhythmia. In their studies the response of action potential duration (APD) during a premature stimulus was measured by high-resolution action potential mapping with voltage-sensitive dyes on a limited area of epicardium of guinea pigs. Their study revealed that when the coupling interval of the premature stimulus was shortened, the pattern of depolarization remain grossly unchanged, while the ventricular gradient was inverted at a critical interval, i.e. the longest AP duration during baseline pacing became the shortest during the premature beat, and vice versa. The phenomenon was explained on the basis of APD restitution kinetics.

In our study the comparison of the QRS and QRST integral maps of naturally evoked premature beats suggests, that the restitution kinetics studied in a small epicardial area [Laurita et al., 1996] should be similar in the whole myocardium. According to [Laurita et al., 1996], the inversion of the APD gradients was about 160° on the epicardial surface of guinea pig ventricle. In the record of our patient shown in Fig. 5 the angle of APD inversion estimated from our values (Fig. 7) was near to 160° as well. Since the angle is influenced by the total ventricular mass according to the physical meaning of eqs.1 and 2, the mechanism and also the degree of inversion should be similar in humans and also in the whole ventricular myocardium.

Fig. 7 shows RR, and NDI values beat-by-beat for premature cycles originating from the same ectopic focus. The different isolated premature beats were always placed in the middle of the graph, consequently the average tendency of the parameter values of beats preceding and following the stimulus are also shown. According to this observation, the NDI of the premature stimuli had a minimum, and the maximal NDI was always found immediately after the premature stimuli. However the scattering of the NDI data suggests that the increase in repolarization disparity is only marginal in several beats. Interestingly, records like Fig. 6 consistently show that extreme values in NDI time-series are not necessarily coinciding with the premature stimuli. Consequently we may hypothesize that dispersion modulation produced by premature stimuli is not the only reason in provoking reentrant arrhythmia.

5. Conclusions

QRS and QRST integral maps provide an insight in the modulation of ventricular depolarization and repolarization spontaneously or by premature stimuli. The same methodology provides tools for the detailed and noninvasive study of the association of repolarization and depolarization sequences as well. According to our preliminary findings, map-type studies, but even simplified studies based on NDI parameters offer an unexplored source of information in the study of arrhythmia v ulnerability.

Acknowledgements

This study was supported by the National Research Found grants NKFP 2/052/2001 and IKTA 142/2002 of the Ministry of Education, Hungary.

References

Cuppen JJ, van Oosterom A. Model studies with the inversely calculated isochrones of ventricular depolarization. *IEEE Trans Biomed Eng*, 31(10): 652-659, 1984.

De Ambroggi L, Aime E, Ceriotti C, Rovida M, Negroni S. Mapping of ventricular repolarization potentials in patients with arrhythmogenic right ventricular dysplasia: principal component analysis of the ST-T waves. *Circulation*, 96(12): 4314-4318, 1997.

Gepstein L, Hayam G, Ben-Haim SA. Activation-repolarization coupling in the normal swine endocardium. *Circulation*, 96(10): 4036-4043, 1997.

Geselowitz DB. The ventricular gradient revisited: relation to the area under the action potential. *IEEE Trans Biomed Eng*, 30(1): 76-77, 1983.

Gulrajani RM. Bioelectricity and Biomagnetism. J. Wiley, New York, 1998.

Laurita KR, Girouard SD, Rosenbaum DS. Modulation of ventricular repolarization by a premature stimulus. *Circ Res*, 79(3): 493-503, 1996.

Laurita KR, Girouard SD, Akar FG, Rosenbaum DS. Modulated dispersion explains changes in arrhythmia vulnerability during premature stimulation of the heart. *Circulation*, 98(24): 2774-2780, 1998.

Lombardi F. Chaos theory, heart rate variability, and arrhythmic mortality. *Circulation*, 101(1): 8-10, 2000.

Lux RL, Smith CR, Wyatt RF, Abildskov JA. Limited lead selection for estimation of body surface potential maps in electrocardiography. *IEEE Trans. Biomed Eng*, 25(3): 270-276, 1978.

Marenco JP, Nakagawa H, Yang S, MacAdam D, Xu L, He DS, Link MS, Homoud MK, Estes III NA, Wang PJ. Testing of a new T-wave subtraction algorithm as an aid to localizing ectopic atrial beats. *Ann. Noninvasive Electrocardiol*, 8(1): 55-59, 2003.

Mitchell LB, Hubley-Kozey CL, Smith ER, Wyse DG, Duff HJ, Gillis AM, Horacek BM. Electrocardiographic body surface mapping in patients with ventricular tachycardia. Assessment of utility in the identification of effective pharmacological therapy. *Circulation*, 86(2): 383-393, 1992.

Nadeau R, Ackaoui A, Giorgi C, Savard P, Shenasa M, Page P. PQRST isoarea maps from patients with the WPW syndrome: an index for global alterations of ventricular repolarization. *Circulation*, 77(3): 499-503, 1988.

Shimizu S, Kobayashi Y, Miyauchi Y, Ohmura K, Atarashi H, Takano T. Temporal and spatial dispersion of repolarization during premature impulse propagation in human intact ventricular muscle: comparison between single vs double premature stimulation. *Europace*, 2(3): 201-206, 2000.

Sippensgroenewegen A, Mlynash MD, Roithinger FX, Goseki Y, Lesh MD. Electrocardiographic analysis of ectopic atrial activity obscured by ventricular repolarization: P wave isolation using an automatic 62-lead QRST subtraction algorithm. *J Cardiovasc Electrophysiol*, 12(7): 780-790, 2001.

Surawicz B. Will QT dispersion play a role in clinical decision-making? *J Cardiovasc Electrophysiol*, 7(8): 777-784, 1996.